
Observations from the Solar Maximum Mission

Keith T. Strong

Phil. Trans. R. Soc. Lond. A 1991 **336**, 327-337

doi: 10.1098/rsta.1991.0084

Email alerting service

Receive free email alerts when new articles cite this article - sign up in the box at the top right-hand corner of the article or click [here](#)

To subscribe to *Phil. Trans. R. Soc. Lond. A* go to:

<http://rsta.royalsocietypublishing.org/subscriptions>

Observations from the *Solar Maximum Mission*

BY KEITH T. STRONG

Lockheed Solar and Astrophysics Laboratory, 3251 Hanover Street, Palo Alto, California 94304, U.S.A.

After nearly a decade of flare observations from the *Solar Maximum Mission (SMM)*, the time has come to pause to review what has been accomplished and to identify the problems that remain to be solved. *SMM* has not only produced a comprehensive database on a variety of active-Sun phenomena but also taught us how to coordinate observations with ground-based observatories and other spacecraft to produce a more holistic view of the complex energy release and transport processes that we call a flare. *SMM* had a unique combination of four imaging instruments which emphasized the spectroscopy of the solar atmosphere. They were the Hard X-ray Imaging Spectrometer, the Bent Crystal Spectrometer, the Flat Crystal Spectrometer, and the Ultraviolet Spectrometer/Polarimeter. To illustrate the power of these instruments, this paper will describe the results of various studies of energy release, transport, and deposition phenomena during the onset of flares.

1. Introduction

A flare is the sudden, catastrophic release of stored magnetic energy in the atmosphere of the Sun. The interplay of the titanic forces unleashed by flares makes them a fascinating plasma laboratory, and it is observations of flares that may eventually lead to a better understanding of the significant underlying physics.

The flare produces rapid increases in electromagnetic radiation from gamma rays to radio wavelengths. The broad range of emissions indicates that a tremendously complex series of physical processes are occurring as a result of the conversion, transport, deposition and dissipation of flare energy. We rely entirely on the radiative signature of these processes to tell us what is happening in the flare plasma. However, some of these processes may not have a radiative signature, and so their presence must be inferred from the well-observed stages of the flare. In these cases we must use our knowledge of the likely physical process in terms of theoretical models to fill in the gaps in observations.

The results from *Skylab* (Sturrock 1980) helped us to formulate many of the fundamental questions associated with active-Sun phenomena that we are still trying to solve today. The *Solar Maximum Mission (SMM)* was the direct result of *Skylab*'s success. *SMM* lacked the high spatial resolution of *Skylab*, but the seven instruments on *SMM* emphasized spectroscopy over a wide range of wavelengths and hence could provide data on the physical parameters throughout the solar atmosphere that were not previously available. The purpose of this paper is to review some of the flare observations made by the four pointed instruments on *SMM*. They were: the Hard X-ray Imaging Spectrometer (HXIS) (van Beck *et al.* 1980); the Bent Crystal Spectrometer (BCS) (Acton *et al.* 1980); the Flat Crystal Spectrometer (FCS)

Phil. Trans. R. Soc. Lond. A (1991) **336**, 327–337

Printed in Great Britain

327

Table 1. *SMM* instrument parameters

parameter	HXIS	BCS	FCS	UVSP
field of view	2.5, 6 arcmin	6 arcmin	0.25–7 arcmin	0.05–4 arcmin
spatial resolution	8, 32 arcsec	6 arcmin	15 arcsec	3 arcsec
spectral coverage	3–30 keV	1.7–3.3 Å	1.5–23 Å	1200–3600 Å
spectral resolution	6	5000–14000	1000–25000	100000
time resolution	1.5–7 s	0.1–11 s	≥ 0.256 s	0.064 s

(Acton *et al.* 1980); and the Ultraviolet Spectrometer/Polarimeter (uvsp) (Woodgate *et al.* 1980).

The basic characteristics of these instruments are summarized in table 1. Between them, *SMM*, *P78-1*, and *Hinotori* covered most of the peak and decay of cycle 21, as well as the spectacular onset of cycle 22. These data represent a unique resource, which will make it possible to study the evolution of the most significant active regions and flares that the Sun produced during this last decade. Although many of the fundamental flare questions remain unsolved, *SMM* has proved to be a catalyst for significant advances in both observation and theory in most areas of flare research, especially for studies of their impulsive phase. It would not be possible in the available space to review all the flare results from these instruments. Consequently, this paper will illustrate how observations from a wide wavelength range can be combined to improve our understanding of the early stages of flares. In particular, long duration events (LDES) and flares associated with coronal mass ejections (CMEs) will be used as examples because their temporal and spatial scales are large and so the onset phase is easier to observe.

2. Observations of energy release processes

It was clear from the early soft X-ray images of the solar corona taken by rockets (Vaiana *et al.* 1973), and later confirmed by *Skylab* (Vaiana & Rosner 1978), that the structure of the corona is dominated by magnetic fields. The magnetic field confines the plasma and may well provide the heating mechanism for maintaining the high-temperature coronal plasma. In the last decade, our ability to reconstruct the geometry of the magnetic field has been vastly improved by the advent of the vector magnetograph. Studies comparing the shear of the field lines with respect to the magnetic inversion line and flare sites (Hagyard *et al.* 1982; Hagyard 1991) have led to the conclusion that the relaxation of these non-potential geometries is the energy source for most flares. There has been little convincing evidence of a substantial change in the observed fields as a result of even major flares. Estimates of the free (available) magnetic energy show that it is generally large compared with the flare energy (see, for example, Strong *et al.* 1984; Gary *et al.* 1987). Hence only a small fraction has to be released to account for the flare, and so little overall change in the field would be observed.

The nature of the instability that triggers the energy release is unknown. The problem is in driving the reconnection process fast enough to produce the explosive energy release that we call a flare. Observing the instability and initial energy release processes directly is difficult because their radiation signatures, if present, are likely to be faint. The timescales are very rapid, so there is little opportunity for an imaging instrument to locate the energy release site or to integrate long enough to obtain

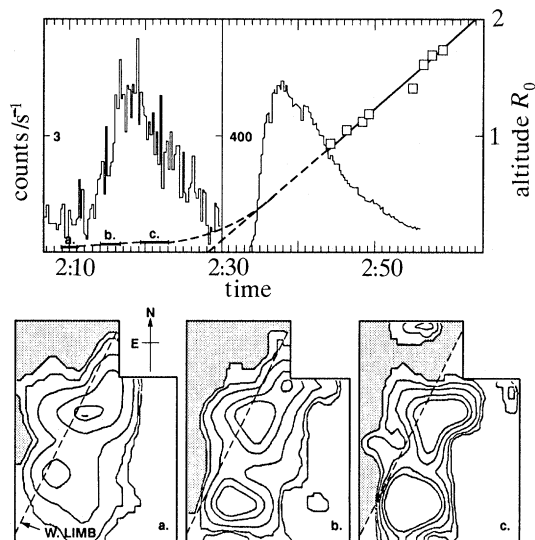


Figure 1. HXIS data from 29 June 1980 flares. The light curves show that there is a faint precursor at the onset time of the CME (from the projection of its trajectory (\square)). In the series of three HXIS images the location of the precursor is seen to be on the southwest limb of the Sun, and it rises throughout the event (from Harrison *et al.* 1985).

meaningful plasma diagnostics. The spatial scale of the initial energy release site is probably well below the resolving power of the *SMM* instruments. However, LDES and CME-related flares have large spatial scales and long timescales, which make them ideal targets for the study of the initial phase of flares.

In a simplified scenario for a CME-related flare, confining coronal field lines become opened as a filament erupts and the CME is launched. The associated flare is the result of the energy released by reconnection of the open field lines as they pinch below the rising filament. The field relaxes to a potential state or, at least, to a lower-energy state releasing free magnetic energy. Observations have shown that the launch of the CME precedes the main phase of the flare (see, for example, Jackson 1981). Hence, the CME could be considered to be the trigger of the flare or, alternatively, the flare could be merely the aftermath of the CME. However, this begs the question of the nature of the instability that caused the launch of the CME.

If the trajectory of the CME is projected back to the photosphere, the approximate time of its launch can be estimated. Harrison *et al.* (1985) discovered from HXIS data that a faint hard X-ray precursor often preceded the main phase of the CME-related flare by 20–30 min, corresponding approximately to the launch time (see figure 1). It is difficult to justify the association of the precursors with the launch time of the CME solely on the basis of time coincidence. There are many such faint brightenings in flare-productive active regions. The launch time is calculated by making assumptions about the CME launch height and acceleration of the CME when it was below the occulting disc of the *SMM* Coronagraph/Polarimeter (CP). The association becomes more compelling when HXIS images are used. These images show that the precursor is located at or near the base of the coronal structure associated with the CME and that its centroid seems to rise (figure 1*a–c*). Simnett & Harrison (1985) show that these brightenings can originate from two or more well-separated sites, presumably opposite ends of the large-scale coronal structure that erupts, causing the transient.

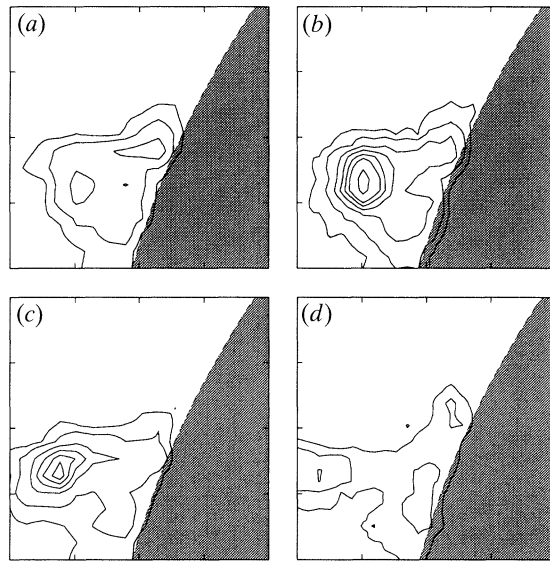


Figure 2. A sequence of four FCS CME-related flare images taken in Fe^{XVII} (15.01 \AA) on 17 October 1986. The images were taken during (a) the onset of the flare at 04:06 UT; (b) the peak of the flare at 04:48 UT; (c) the decay phase of the flare 05:54 UT and (d) 07:42 UT. The solar disc is indicated by the shaded area. The contour levels correspond count rates of 50, 100, 200, 300, 400, 500 and 800. Each image is 4 arcmin square.

Figure 2 shows an LDE that was associated with a faint CME. It was a C3 GOES-level flare which started at 04:00 UT on 17 October 1986 and lasted for about 16 h. The parent active region was located on the north-eastern limb of the Sun, so the FCS could map the height structure of the flare. The first FCS images were taken in Fe^{XVII} (at 15.01 \AA) during the flare onset (figure 2a), peak (figure 2b), and decay (figure 2c, d). These data clearly show a large bright volume of plasma initially at about 50000 km above the solar limb. In the subsequent images, this bright X-ray source moved out radially at an average velocity of about 4 km s^{-1} . Flare loops were plainly visible beneath this bright volume. Both of these components are initially about equal in intensity, but later in the flare the high coronal source dominates. It is tempting to identify the bright X-ray source as a reconnection site identified in the above scenario. The flare loops occur because energy released during that reconnection process is trapped in the (now) closed magnetic field lines. Hence the images, taken by themselves, are consistent with the model.

For this event, the FCS also made extensive spectral scans at the brightest pixel in the coronal X-ray source soon after the peak of the flare and there were a series of UVSP images showing the location of the sunspots as they rotated over the limb. Unfortunately, there were no BCS data for this event. Results from analysis of these spectra indicate that the characteristic electron temperature (from $\text{Fe}^{\text{XVII}}:\text{Fe}^{\text{XVIII}}$ and $\text{Mg}^{\text{XI}}:\text{Mg}^{\text{XII}}$ line ratios) is about $6 \pm 2 \text{ MK}$, although the plasma is clearly not isothermal. A differential emission measure model, derived from 45 soft X-ray line intensities, shows a broad distribution between 4 and 10 MK (J. T. Schmelz, personal communication). The electron density, determined from the total emission measure and an estimated volume, is about 10^{10} cm^{-3} for a uniformly filled coronal volume (i.e.

$$\dagger 1 \text{ \AA} = 10^{10} \text{ m} = 10^{-1} \text{ nm.}$$

no filamentation). This is a surprisingly large value for such a great height in the corona. Possibly the most intriguing aspect of the FCS spectra is the measurement of the dynamics of the plasma derived from shifts and broadening of the Mg^{XI} line at 9.17 Å (J. L. R. Saba, personal communication). These data show the X-ray lines to be consistent with their thermal widths; i.e. there are no significant turbulent motions or flows above about 20 km s⁻¹ (the FCS limit). This is most unusual, especially for flare plasma, in which mass motions are generally over 100 km s⁻¹. Hence, it seems unlikely that this is a site for continuous energy release.

From the X-ray images and the physical parameters derived from the spectra, it is possible to estimate the relative amount of thermal energy in the plasma at various heights (i.e. times) in the corona. If this were just a simple reconnection event, one might expect the energy released (E) to be proportional to the square of strength of the magnetic field (B), as $E = (B^2 - B_0^2)/8\pi$, where B_0 is the strength of the equivalent potential field. For a simple dipole, the magnetic field strength falls off as the cube of the height (h), so the energy released in the corona would vary as h^{-6} . For a more complex geometry, such as an arcade, the field strength falls as h^2 , so the energy released would vary as h^{-4} . However, the observed rate of decrease of the thermal energy varies as about h^{-3} . This result implies that the rising bright X-ray source is unlikely to be a reconnection site unless the region has an exotic magnetic structure.

Alternatively, the coronal source could be hot plasma isolated from the lower levels of the atmosphere by the pinching off of field lines. This can be tested by calculating the radiative cooling time (τ_r), where $\tau_r = E_{\text{th}}/VP_{\text{rad}} \approx 222 T_6^{5/2} n_{10}^{-1}$ (Raymond *et al.* 1976; Rosner *et al.* 1978), where V is the plasma volume (cm³), P_{rad} is the radiative loss rate (erg s⁻¹ cm⁻³†), T_6 is the electron temperature (MK), and n_{10} is the electron density (10¹⁰ cm⁻³). If the measured temperatures and densities are substituted in this expression, the radiative cooling time is calculated to be about 4500 s. The observed cooling time is about 5700 s. Within the uncertainty of the respective calculations, these two values are comparable. Hence, if there is any long-term energy release in the coronal source region, it must be relatively small and will not be a major contributor to the flare emission.

3. Observations of energy transport and deposition

A source of some controversy has been whether conduction fronts or accelerated particles carry the bulk of the energy away from the energy release site. Observations, particularly from the *SMM* Hard X-ray Burst Spectrometer (HXRBS) and γ -ray spectrometer (GRS), as well as from the imaging instruments, have generally supported the particle acceleration models to the extent that the burden of proof now lies on those supporting the conduction front model.

The first contribution to this view to come from *SMM* observations was from HXIS. Hoyng *et al.* (1981) pointed out that the hard X-ray emission came first from the footpoints of the flare loops. A more extensive study by Duijveman *et al.* (1982) showed that within a few minutes the emission shifted from the footpoints to a point between them, presumably the apex of the loop (see figure 3). These observations were interpreted as evidence for thick-target emission from electron bremsstrahlung caused by an electron beam accelerated at the energy release site in the corona. However, this footpoint structure was detected in only a few flares. This may be just

† 1 erg = 10⁻⁷ J.

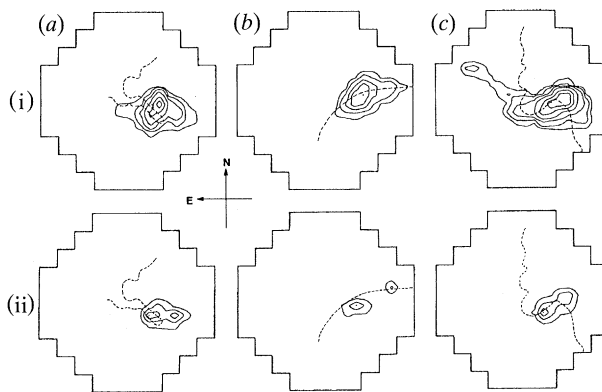


Figure 3. The impulsive phase of three flares imaged by the *HXIS* (i) low-energy channel (3.5–5.5 keV) and (ii) the sum of the two high-energy channels (16–30 keV). The dashed lines indicate the location of the magnetic inversion line. Note how there seems to be a bright point on either side of the neutral line in the 16–30 keV images but in the 3.5–5.5 keV images the bright area spans the neutral line (from Duijveman *et al.* 1982). (a) 10 April 1980, 09:18:38 UT; (b) 21 May 1980, 20:55:55 UT; (c) 5 November 1980, 22:33:05 UT.

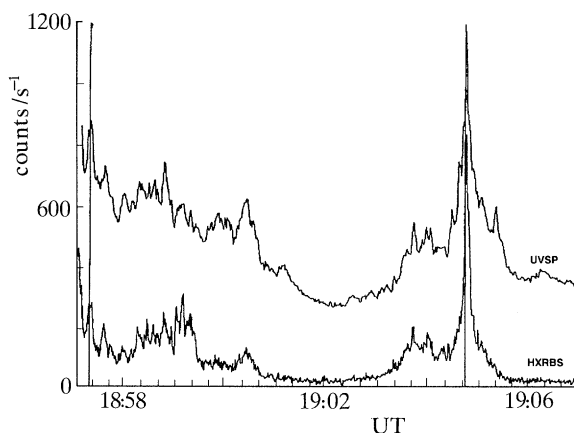


Figure 4. The lightcurve of the impulsive phase emissions observed by *UVSP* (upper curve) and *HXRBS* (lower curve) from a flare on 8 March 1989. Note the close correspondence between the timing of individual bursts.

an instrumental threshold effect or a genuine difference between flares, but it means that these results alone cannot resolve the issue.

Unfortunately, *HXIS* was operational only in 1980, so *SMM* lost the capability to directly image the hard X-ray sources after its repair in 1984. However, it was discovered that *UV* line and continuum light curves closely follow the hard X-ray burst time profile during the impulsive phase of flares (Poland *et al.* 1982; Orwig & Woodgate 1986). In figure 4 some *UV* bursts are obviously correlated with hard X-ray spikes. The simultaneity of the burst (less than 1 s) implies that the hard X-ray burst and *UV* signal are produced at the same site, namely in the chromosphere, presumably as a result of a particle beam. However, there is not a simple correspondence between the size and relative timing of all the bursts. These discrepancies could be accounted for partially by difference in the fields of view of

HXIS and HXRBS. Recent work by R. Schwartz and S. Drake (personal communication) has shown that the sources are compact (less than 10 arcsec) and that the individual bursts come from many different locations. The discovery of this UV/hard X-ray correspondence has led to the intriguing possibility of imaging the location of the hard X-ray burst by using UV emission as a surrogate.

These results have added to the growing body of evidence that particle beams play the major role in energy transport in the impulsive phase of flares. Are there any counter examples? The 17 October 1986 LDE (see above) would seem to be the ideal candidate to examine for a thermal conduction front as the initial energy transport mechanism. The timescale of the rise was long (about 30 min), and there was no significant hard X-ray burst, so particles are not needed to account for rapid timescales or impulsive-phase bursts. The FCS observed a large volume of dense thermal plasma at the apex of the loop. However, it is interesting that in the initial image (figure 2a) the loop brightening is asymmetric, with its northern leg being significantly brighter along most of its length below the source region. A conduction front should produce a symmetric brightening in the loop if, as seems to be the case, the energy is being released at the loop apex.

A particle acceleration model could explain the asymmetry in the loop more easily by using magnetic mirroring. Particles can be mirrored by strong, converging magnetic fields, if their pitch angle is larger than a critical value and if the ambient plasma density at the mirror point does not become high enough to make collisions likely. Hence, a larger proportion of the particles carrying the flare energy could be mirrored while still in the tenuous corona or transition region at the footpoint where the field is strongest. UVSP continuum images show that the sunspots were beneath the southern (fainter) leg of the loop. No major spots were visible at the northern end of the arcade. Therefore, we could reasonably expect the field to be strongest at the southern end of the loop and hence some portion of the particles there to be mirrored, while most of the particles moving down toward the magnetically weaker (northern) footpoint would be absorbed into the chromosphere, where they deposit their energy. The mirrored particles would then travel back along the length of the loop and could lose their energy as they, too, plunge into the denser chromosphere at the northern footpoint. This would produce the observed asymmetry in the brightening of the corona as the explosively heated plasma flowed back up into the corona. The intensity contrast between the two loop legs is a factor of 2–3, which would require 30–50% of the particles in the southern loop leg to be mirrored and deposited at the other footpoint.

If the flare energy is released in the corona and transported along the magnetic field lines to be deposited in the dense chromosphere almost instantaneously, the chromosphere would not have time to conduct or radiate away the excess energy; this would cause an explosive evaporation (or ablation) of the chromospheric plasma up into the corona. If the bright emission at the northern leg of the loop is evaporating chromosphere material, then the velocity of the upflowing plasma is between 120 and 250 km s⁻¹ (derived from the angular rate at which the FCS maps from west to east and the onset time from *GOES*). These mass motions are consistent with those seen in many other flares (see, for example, Doschek *et al.* 1980; Antonucci *et al.* 1982, 1984; Fludra *et al.* 1989). These mass motions are the result of energy deposition in the chromosphere and represent a different form of energy transport. They also act as temporary storage for some of the flare energy, which later can be thermalized by collisions in the corona. VCS observations can be used to quantify the turbulent

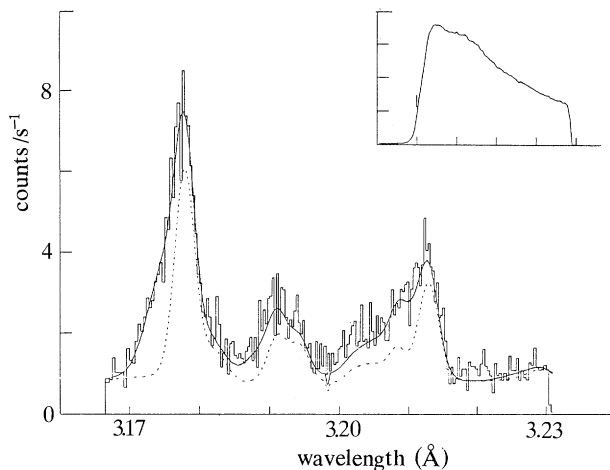


Figure 5. An example of line broadening as seen by the BCS in Ca^{XIX} during the impulsive phase of a flare that occurred on 8 April 1980 at 03:05 UT. The data are plotted as a histogram, superimposed on that is a two component fit (solid line) to the spectrum; the stationary component is marked with a dashed curve. The time of the spectrum is marked on the light curve (upper right) with a dash (from Fludra *et al.* 1989).

and direct flows of the flare plasma ($T_e \geq 10$ MK). Typical values for the upflows are between 200 and 400 km s^{-1} , and the lines are broadened by about 100–200 km s^{-1} (see figure 5). However, when such flows are seen from a strongly blue-shifted component in the X-ray line profiles, there is also a significant stationary component. The question of whether the integral over time of the mass of the evaporating plasma is sufficient to supply the mass of stationary plasma has been the subject of much debate (Doschek *et al.* 1984). The data seem to be insufficient to resolve this problem and we may have to wait for the increased sensitivity of *Solar-A* to provide an answer.

The nature of the line broadening, often referred to as turbulence, during the early stages of flares is also of great interest. Although macroscopic turbulence is not possible in the corona owing to the confining influence of the magnetic field, small-scale plasma turbulence could be the source of the observed line broadening. Doyle & Bentley (1986) found some tantalizing evidence of discrete blue-shifted and red-shifted components at the onset of some flares, which implies that the broadening may be a result of a distribution of line shifts around the rest wavelength. However, these data were at the very limit of detectability for the BCS and will require more sensitive measurements before they can be confined.

Coronal density diagnostics are rarely available. Linford & Wolfson (1988) studied a very impulsive C3 flare in which they found coronal densities of about $4 \times 10^{12} \text{ cm}^{-3}$ during the rise of the flare by using FCS spectra of the He-like Mg^{XII} triplet. These data, combined with high-resolution $\text{H}\alpha$ images, enabled them to determine the volume and hence the diameter of the flare loop. The loop was found to be only 150 km in diameter ($\equiv 0.2$ arcsec) and 20 000 km long. This result demonstrates the extreme fine structure that may exist in some flares, in contrast to that of the LDES, as well as the power of spectral diagnostics that makes it possible to determine spatial scales below the theoretical resolution of the instrument (15 arcsec for the FCS). Unfortunately, this diagnostic is useful only for the plasma at about 5 MK. The

only density diagnostic available for the flare plasma above 10 MK is the time the plasma takes to reach equilibrium (Mewe *et al.* 1985); there are no convincing examples of such conditions existing during the impulsive phase of flares, probably because of the lack of sensitivity and time resolution of existing instruments.

The relative importance of the energy stored in the bulk motions is an open issue. The lack of high spatial resolution or reliable density diagnostics for the hot flare plasma makes determination of the kinetic energy and momentum balance (Canfield *et al.* 1987) sufficiently uncertain that definitive conclusions are hard to justify. With reasonable assumptions for the filling factor of the coronal plasma (*ca.* 0.01) for a few selected impulsive flares, the energy in the accelerated particles and the bulk motions, and the thermal energy are similar (Wu *et al.* 1984). In comparing the energy of a particle beam with the energy in the thermal flare, the major source of uncertainty is the low-energy cut-off of the particles. A small change in the cut-off energy can result in a large change in the energy of the beam. Generally, a cut-off of about 25 keV is assumed for no particularly physical reason except that it gives about the right amount of energy! This is an area where progress can be made with data from the Gamma Ray Observatory (GRO) in conjunction with future solar missions.

Unfortunately, determining the energetics of the impulsive phase is a very difficult problem. Strong *et al.* (1984) looked at the detailed energetics of a double impulsive flare by using data from ten different *SMM* and ground-based instruments. The interesting aspect of these observations was that the energetics of the two events were completely different, although they came from the same active region and occurred only 150 s apart. The hard X-ray burst in the first event was relatively strong and produced a *GOES* C3 flare. The second event had a much weaker hard X-ray burst, although it lasted longer and had a similar total energy in the electron beam, but produced an M2 flare (i.e. nearly seven times more thermal plasma for the same energy input). This presents us with a problem if the thermal energy in the flare is a direct result of the energy deposited in the chromosphere. Only by combining data from a variety of instruments (from radio to hard X-rays) did there seem to be a self-consistent solution, namely that the two flares occurred in the same plasma volume: thus the second event dumped its energy into hot, ionized plasma, causing there to be a lower yield of hard X-rays (Brown 1973) and heating the plasma to a higher temperature (as it was already hot), hence making it more emissive at the relevant soft X-ray wavelengths. Without this array of instrumentation, this event could have been considered as providing evidence for the decoupling of the impulsive and gradual phases.

4. Conclusions

As the above examples demonstrate, there are dangers in looking at single events or at data from individual instruments in isolation. The *LDE* observations show that the location of the primary energy release site is the corona and that the energy is probably transported by accelerated particles to the chromosphere. However, how representative is this event of other *LDEs* or of flares in general? We must avoid generalizing too broadly from these relatively rare events to draw fundamental conclusions about all flares. The geometry and timescales are unique to this type of event, and consequently they are possibly not representative of the general conditions in flares, although they may have some physical processes in common. The *SMM* flare analysis so far has concentrated on a few tens of large (M and X) flares. Very little work has been done on C flares although they make up a majority

of the flares observed. If we concentrate on just the spectacular flares, we will arrive at a distorted or even incorrect view of flare processes. We need to study flares on many different spatial, temporal and intensity scales. Statistical studies of a full range of flares and their relation to the structure and evolution of their parent active regions may lead to reliable ways of classifying and predicting flares.

There is a wealth of *SMM* data that has not been analysed, especially by an integrated approach as discussed above. About a third of the flares (over 10000) observed in the lifetime of the *SMM* satellite were observed in the last 18 months and have not been scientifically evaluated. Although bringing disparate data together can be time consuming and often frustrating, it is certainly worth the effort. It is clear that we need to be able to derive more accurate and reliable plasma diagnostics on small spatial scales than have been possible to date. The next decade holds bright prospects for solar physics with the launch of *Solar-A* during the decay of solar cycle 22. Later we will have the results from the Solar Heliographic Observatory and, hopefully, Orbiting Solar Laboratory by the end of the decade. The scientific goals of these missions will be built on the foundations laid in the 1970s by *Skylab* and in the 1980s by *SMM*, *Hinotori*, and *P78-1*. It promises to be a very exciting decade in solar physics.

References

- Acton, L. W. *et al.* 1980 The soft X-ray polychromator for the *Solar Maximum Mission*. *Solar Phys.* **65**, 53–71.
- Antonucci, E., Gabriel, A. H., Acton, L. W., Culhane, J. L., Doyle, J. G., Leibacher, J. W., Machado, M., Orwig, L. E. & Rapley, C. G. 1982 Impulsive phase of flares in soft X-ray emission. *Solar Phys.* **78**, 107.
- Antonucci, E., Gabriel, A. H. & Dennis, B. R. 1984 The energetics of chromospheric evaporation in solar flares. *Astrophys. J.* **287**, 917.
- Brown, J. C. 1973 *Solar Phys.* **32**, 227.
- Canfield, R. C., Metcalf, T. R., Strong, K. T. & Zarro, D. M. 1987 A novel observational test of momentum balance in a solar flare. *Nature* **326**, 185.
- Doschek, G. A. *et al.* 1984 *Energetic phenomena on the Sun*, ch. 4, Proc. *Solar Maximum Mission Workshop* (ed. M. R. Kundu & B. Woodgate), NASA CP 2439.
- Doschek, G. A., Feldman, U., Kreplin, R. W. & Cohen, L. 1980 *Astrophys. J.* **239**, 725.
- Doyle, J. G. & Bentley, R. D. 1986 Broadening of soft X-rays lines during the impulsive phase of solar flares: random of direct motions. *Astron. Astrophys.* **155**, 278.
- Duijveman, A., Hoyng, P. & Machado, M. E. 1982 X-ray imaging of three flares during the impulsive phase. *Solar Phys.* **81**, 137.
- Fludra, A., Lemen, J. R., Jakimec, J., Bentley, R. D. & Sylwester, J. 1989 Turbulent and directed plasma motions in solar flares. *Astrophys. J.* **344**, 991–1003.
- Gary, G. A., Moore, R. L. & Hagyard, M. J. 1987 Non-potential features observed in the magnetic field of an active region. *Astrophys. J.* **314**, 782–794.
- Hagyard, M. J. 1991 The significance of vector magnetic field measurements. *Memorie della Società Astronomica Italiana. Solar Magnetic Fields* (ed. G. Poletto). (In the press.)
- Hagyard, M. J., Cuming, N. P., West, E. A. & Smith, J. E. 1982 The MSFC vector magnetograph. *Solar Phys.* **80**, 33–51.
- Harrison, R. A., Waggett, P. W., Bentley, R. D., Phillips, K. J. H., Bruner, M., Dryer, M. & Simnett, G. 1985 The X-ray signature of coronal mass ejections. *Solar Phys.* **97**, 387–400.
- Hoyng, P., Machado, M. E., Duijveman, A., Boelee, A., de Jager, C., Frost, K. J., Lafleur, H., Simnett, G. M., van Beek, H. F. & Woodgate, B. E. 1981 Origin and location of the hard X-ray emission in a two-ribbon flare. *Astrophys. J. Lett.* **246**, L155.
- Jackson, B. V. 1981 Forerunners: early coronal manifestations of solar mass ejections. *Solar Phys.* **73**, 133–144.

- Linford, G. A. & Wolfson, C. J. 1988 Properties of an impulsive compact solar flare determined from *Solar Maximum Mission* X-ray measurements. *Astrophys. J.* **331**, 1036–1046.
- Mewe, R., Lemen, J. R., Peres, G., Schrijver, J. & Serio, S. 1985 Solar X-ray simulations for flaring loop models with emphasis on transient ionisation effects during the impulsive phase. *Astron. Astrophys.* **152**, 229.
- Orwig, L. E. & Woodgate, B. E. 1986 *The lower atmosphere in solar flares*, pp. 306–317.
- Poland, A. I., Machado, M. E., Wolfson, C. J., Frost, K. J., Woodgate, B. E., Shine, R. A., Kenny, P. J., Cheng, C. C., Tandberg-Hanssen, E. A., Bruner, E. C. & Henze, W. 1982 The impulsive and gradual phases of a solar limb flare as observed from the *Solar Maximum Mission* satellite. *Solar Phys.* **78**, 201–213.
- Raymond, J. C., Cox, D. P. & Smith, B. W. 1976 *Astrophys. J.* **204**, 290.
- Rosner, R., Tucker, W. H., Vaiana, G. S. 1978 *Astrophys. J.* **220**, 643.
- Saba, J. L. R. & Strong, K. T. 1991 Coronal dynamics of a quiescent active region. *Astrophys. J.* (In the press.)
- Simnett, G. & Harrison, R. A. 1985 The onset of coronal mass ejections. *Solar Phys.* **99**, 231.
- Strong, K. T., Benz, A. O., Dennis, B. R., Leibacher, J. W., Mewe, R., Poland, A. I., Schrijver, J., Simnett, G., Smith, J. B., Jr. & Sylwester, J. 1984 A multiwavelength study of a double impulsive flare. *Solar Phys.* **91**, 325–344.
- Storrock, P. A. (ed.) 1980 *Solar flares: a monograph from Skylab solar workshop*. Colorado Associated University Press.
- Vaiana, G. S., Krieger, A. S. & Timothy, A. F. 1973 Identification and analysis of structures in the corona from X-ray photography. *Solar Phys.* **32**, 81–116.
- Vaiana, G. S. & Rosner, R. 1978 Recent advances in coronal physics. *A. Rev. Astron. Astrophys.* **16**, 393–428.
- van Beck, H. F., Hoyng, P., Lafleur, W. & Simnett, G. M. 1980 The hard X-ray imaging spectrometer (HXIS). *Solar Phys.* **65**, 39–52.
- Woodgate, B. E., Tandberg-Hanssen, E. C., Bruner, E. C., Beckers, J. M., Brandt, J. C., Henze, W., Hyder, C. L., Kalet, M. W., Kenny, P. J., Knox, E. D., Michalitsianos A. G., Rehse, R., Shine, R. A. & Tinsley, H. D. 1980 The ultraviolet spectrometer and polarimeter on the *Solar Maximum Mission*. *Solar Phys.* **65**, 73–90.
- Wu, S. T. *et al.* 1984 *Energetic phenomena on the Sun*, ch. V, Proc. *Solar Maximum Mission* Workshop (ed. M. R. Kundu & B. Woodgate), NASA CP 2439.

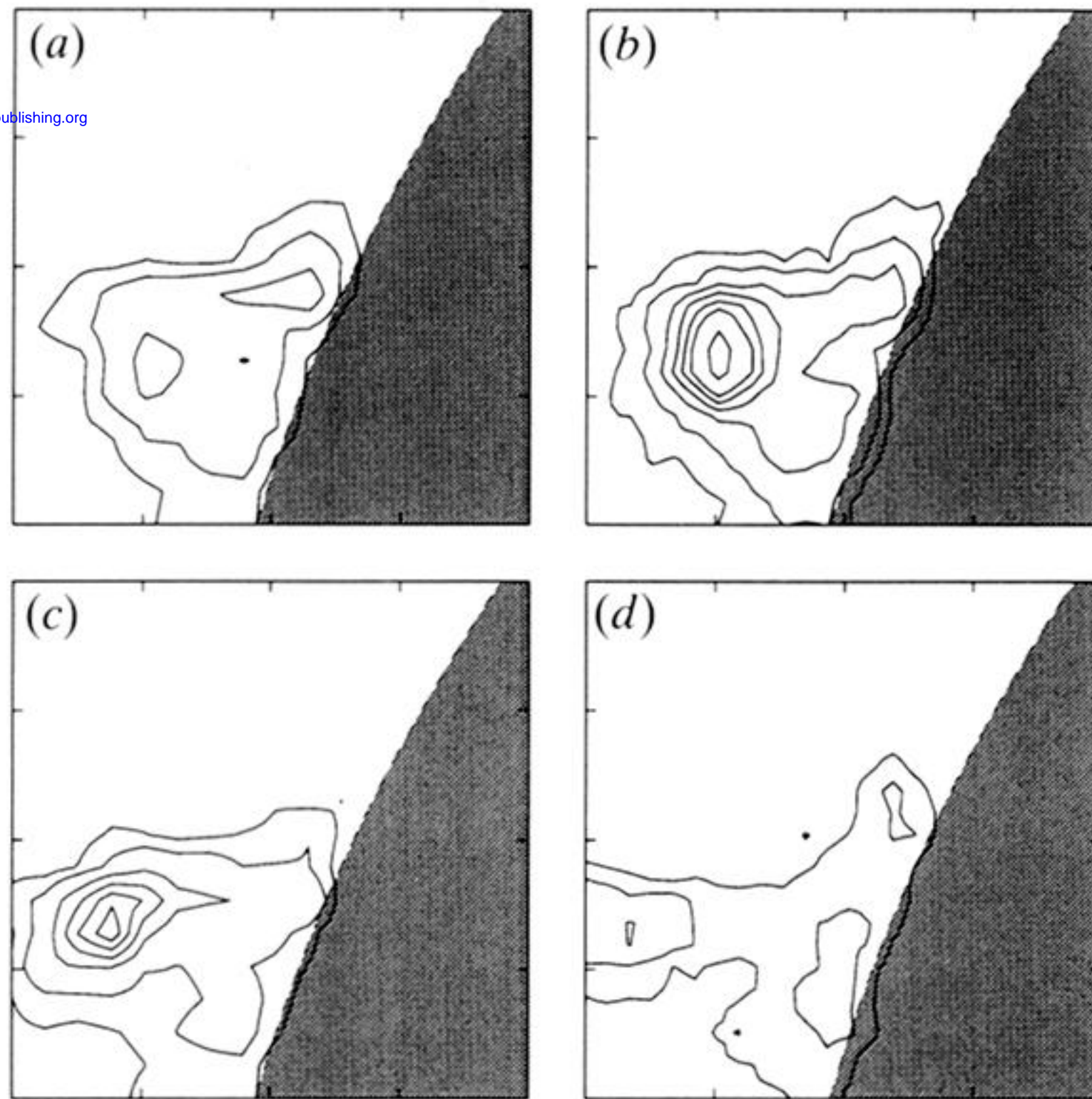


Figure 2. A sequence of four FCS CME-related flare images taken in Fe^{XVII} (15.01 \AA) on 17 October 1986. The images were taken during (a) the onset of the flare at 04:06 UT; (b) the peak of the flare at 04:48 UT; (c) the decay phase of the flare 05:54 UT and (d) 07:42 UT. The solar disc is indicated by the shaded area. The contour levels correspond to count rates of 50, 100, 200, 300, 400, 600 and 800. Each image is 4 arcmin square.